IEEE Access
Multidisciplinary ⋮ Rapid Review ⋮ Open Access Journal

Received 1 July 2024, accepted 20 July 2024, date of publication 30 July 2024, date of current version 11 September 2024.

Digital Object Identifier 10.1109/ACCESS.2024.3435686

RESEARCH ARTICLE

A Modified Thyristor-Based Auto-Passing Neutral Section Scheme With One Auxiliary Transformer

ZHI ZHANG[1], (Member, IEEE), TRILLION Q. ZHENG[2], (Senior Member, IEEE), ZHIBO ZHANG[2], (Graduate Student Member, IEEE), KAI LI[2], (Member, IEEE), AND SILE YANG[1]

[1]Locomotive & Car Research Institute, China Academy of Railway Sciences Corporation Ltd., Beijing 100081, China
[2]School of Electrical Engineering, Beijing Jiaotong University, Beijing 100044, China

Corresponding author: Kai Li (kaili@bjtu.edu.cn)

This work was supported in part by the Key Project of China State Railway Group Corporation Ltd., under Grant N2022J041, and in part by the Key Project of China Academy of Railway Sciences Corporation Ltd., under Grant 2022YJ242.

ABSTRACT The existence of the neutral section is used to be a major problem of the AC electrified railway. Although the conventional thyristor-based auto-passing neutral section schemes allow a train to go through the neutral section with power, there still exists a power interruption time in milliseconds and the issue of the inrush current in the on-board transformer. Aimed at these shortcomings, a modified thyristor-based scheme with one simplified auxiliary transformer is proposed in this paper. By introducing one 3:1 transformer and two additional switches, two transition voltages, whose phases are between that of two power supply arms, are constructed. The neutral section voltage is switched three times when a train passes through so as to avoid the significant voltage phase change on the grid side of the electric locomotive. Meanwhile, the power interruption time can be lowered to hundreds of microseconds and the inrush current of the on-board transformer is effectively avoided. The working principle of the proposed scheme is deeply analyzed and the characteristics are discussed. Further, the effectiveness and superiority of the proposed scheme is verified by the simulation and experimental results. The impact of the neutral section on the train can be well suppressed by the proposed scheme.

INDEX TERMS Auxiliary transformer, flux linkage, neutral section, power interruption time, switch-based scheme.

I. INTRODUCTION

Due to the economic benefits, the 25kV 50Hz single-phase traction power supply system is adopted world-widely for the electrified railway [1]. The three-phase power from the 110- or 220-kV grid is converted to two single phases for the catenary system by the traction transformer [2]. Two segments of catenary on both sides of a traction substation are powered by the two outputs of the traction transformer with a voltage phase difference of 60° or 90°. Accordingly, a neutral section, also referred to as electrical phase separation, is set on the catenary for electrical isolation of two segments.

Since there is no power supply in the neutral section, the train is prohibited from passing with traction current to avoid a serious electric arc. As a result, the interrupted electrical phase separation passing scheme is widely adopted at present. The train would slide across the neutral section by inertia. This scheme is simple and reliable, but it will lead to the issues of speed loss, the electric arc and the transient over-voltage [3]. Especially for the heavy-haul railways, the train may stop in the neutral section due to an insufficient initial speed. In order to avoid these problems, some auto-passing neutral section passing schemes have been proposed. Further, these schemes can be classified into switch-based ones and converter-based ones.

At the beginning, the high-voltage circuit breakers are used in the switch-based scheme [4]. With this scheme, the train speed loss can be significantly reduced. However, it is difficult to precisely control the operation time of high-voltage circuit breakers, which will lead to the serious electric arc and the high resonant overvoltage. Besides, the train still has a power interruption time of several hundred

The associate editor coordinating the review of this manuscript and approving it for publication was Nagesh Prabhu.

milliseconds [5], [6]. In response to the drawbacks of the high-voltage circuit breaker, the electronic switches are applied in the switch-based schemes [7], [8]. Because of the outstanding overcurrent capacity, the natural turning-off characteristic of current zero crossing, and the short-circuit characteristic in broken state, the thyristor is highly favored [9]. Consequently, the power interruption time is further lowered to several milliseconds in addition to suppress the electric arc and the overvoltage. Nevertheless, the dead time of the voltage switching process is inevitable.

With the development of power electronics technology, the converter-based schemes have been researched recently for completely eliminating the power interruption time. The uninterruptible flexible connector with a back-to-back converter is the most typical converter-based scheme [10]. With a variable frequency and phase shift control strategy, the neutral section voltage can be transferred smoothly without power interruption and the impact of the neutral section on the train can be eliminated [11]. However, this scheme requires a large capacity converter with complex control, which results in high cost and low reliability. To reduce the converter capacity, a flexible uninterruptible phase-separation passing device with phase-shifting transformers is presented in [12], but the high-capacity line-frequency transformers need large installation area. In addition, the time of a train passing the neutral section is relatively short, so the equipment utilization rate of the above two schemes is particularly low [13]. For these reasons, the modified scheme based on modular multilevel converter (MMC) is studied in [14] and [15]. It can perform the phase-separation passing function with power supply when a train is passing the neutral section. For the rest of time, it can be used to balance the traction load of different power supply arms and compensate for the reactive power and the harmonics. But the converter capacity in this scheme is still large and more devices are needed. On the other hand, the co-phase traction power supply system is another solution. By transforming the traction power supply system and adding power electronic converters, the voltage phase of the whole railway is consistent and the neutral section on the catenary can be cancelled [16], [17]. Meanwhile, the power quality of the grid can be greatly improved. However, the converter capacity of the co-phase scheme is equal to the total power of all trains in the line. It causes a higher cost than that of the flexible uninterruptible phase-separation passing devices [18].

There is no doubt that these converter-based schemes have an excellent performance, but their application is restricted due to high cost and low reliability [19]. By comparison, the switch-based schemes have much simpler structures and lower cost. However, the shortcomings in the conventional thyristor-based schemes are obvious and non-negligible. In addition to the power interruption time in milliseconds, the neutral section voltage can only be directly switched between two power supply arms, which may affect the phase locked loop (PLL) of the four-quadrant converter (4QC) on the train. Furthermore, an inappropriate operation time of thyristor can cause a huge inrush current. The train operation would be seriously affected. To address these problems, a thyristor-based scheme with two auxiliary transformers and four switches is proposed in [20] to improve the voltage switching process. Although it works well and has strong adaptability, the drawback is that the two three-winding transformers significantly increase the structure complexity and cost.

On this basis, this paper proposes a modified scheme with only one simple transformer. By the cooperation of one 3:1 auxiliary transformer and two additional switches, two transition voltages, whose phases are between that of two feeders, are constructed. When a train is passing the neutral section, the voltage switching process of the neutral section catenary can be smoother through the operation of different switches. The power interruption time can also be controlled to hundreds of microseconds. Meanwhile, according to the simulation and experimental results, the inrush current of the on-board transformer can be effectively avoided.

The rest of this paper is organized as follows: In Section II, the topology and its working principle of the proposed scheme are introduced in detail. Section III analyzes the characteristics of the proposed scheme and the mechanism of avoiding inrush current. The correctness of the theoretical analysis is verified by the simulation results in Section IV and a scaled-down experimental platform is established in Section V and the experimental results are further carried out. Finally, Section VI summarizes this paper.

II. TOPOLOGY AND WORKING PRINCIPLE

A. CONFIGURATION

Fig. 1 illustrates the topology of the proposed thyristor-based scheme. The proposed scheme includes S_a, S_{c1}, S_{c2}, S_b, and one auxiliary transformer, T_a. Therein, all switches are composed of multiple thyristors connected in series and in anti-parallel. AA_0 and BB_0 are two feeders from the traction substation. And the two power supply arms on both sides of the neutral section are respectively powered by A_0A_1 and B_0B_1. S_a, S_{c1}, S_{c2} and S_b are in series connection between A_0A_1 and B_0B_1. The neutral section catenary is connected to the middle of S_{c1} and S_{c2} by the feeder QN. The primary side

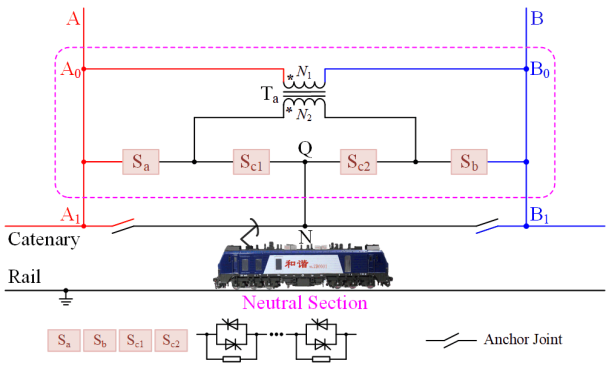

FIGURE 1. Configuration of the proposed scheme.

terminals of T_a are connected to A_0A_1 and B_0B_1, while the secondary side terminals of T_a are connected to the middle of S_a and S_{c1}, and the middle of S_{c2} and S_b, respectively. The turns ratio of T_a is N_1: N_2 = 3:1, and the dotted terminals are marked in Fig. 1 with '*'.

B. WORKING PRINCIPLE

The voltage phase difference between the two outputs of the traction transformer has different situations. The situation of 60° is introduced for the working principle analysis firstly. $\dot{U}_a$, $\dot{U}_b$, and $\dot{U}_n$ are used to represent the voltages of AA_0, BB_0, and the neutral section catenary, respectively. It is assumed that $\dot{U}_a$ leads $\dot{U}_b$ by 60°. For the convenience of analysis, $\dot{U}_a$ and $\dot{U}_b$ are expressed as

$$\begin{cases} \dot{U}_a = U_m\angle 0° \\ \dot{U}_b = U_m\angle -60° \end{cases} \tag{1}$$

where U_m is the rated voltage amplitude of catenary.

Compared to the conventional thyristor-based schemes, S_{c1}, S_{c2} and T_a in Fig. 1 are additional. Due to the introduction of T_a, the voltage phasor of $(\dot{U}_b$-$\dot{U}_a)/3$ is constructed. Further, S_{c1} and S_{c2} are used to realize its calculation with $\dot{U}_a$ and $\dot{U}_b$, so two transition voltages, $\dot{U}_{n1}$ and $\dot{U}_{n2}$ shown in Fig. 2, can be obtained.

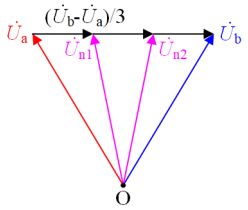

FIGURE 2. Phasor diagram of the proposed scheme.

The process of an electric locomotive passing through the neutral section from AA_0 to BB_0 is analyzed to illustrate the working principle of the proposed scheme. As shown in Fig. 3, the whole process can be divided into 6 states.

1) State I: At the beginning, all switches are in off-state as shown in Fig. 3(a), the neutral section catenary has no power.

2) State II: When the electric locomotive is ready to enter the neutral section, S_a and S_{c1} are switched on. Subsequently, the electric locomotive enters the neutral section with power and $\dot{U}_n$ is equal to $\dot{U}_a$, which is shown in Fig. 3(b).

3) State III: As shown in Fig. 3(c), the electric locomotive arrives at the voltage switching point P. Then S_{c1} is switched off firstly and S_{c2} is switched on later. $\dot{U}_n$ is switched to $\dot{U}_{n1}$, which can be expressed as

$$\dot{U}_{n1} = \dot{U}_a + \frac{1}{3}\left(\dot{U}_b - \dot{U}_a\right) = 0.882U_m\angle -19.1° \tag{2}$$

4) State IV: After several line-frequency cycles, S_a and S_{c2} are switched off firstly, S_b and S_{c1} are switched on later. As shown in Fig. 3(d), $\dot{U}_n$ is switched to $\dot{U}_{n2}$, which can be expressed as

$$\dot{U}_{n2} = \dot{U}_b - \frac{1}{3}\left(\dot{U}_b - \dot{U}_a\right) = 0.882U_m\angle -40.9° \tag{3}$$

5) State V: After a short time, as shown in Fig. 3(e), S_{c1} is switched off firstly and S_{c2} is switched on later, and $\dot{U}_n$ is switched to $\dot{U}_b$.

6) State VI: After the electric locomotive drives out of the neutral section, S_b and S_{c2} are switched off. As shown in Fig. 3(f), the neutral section catenary recovers to the no power state.

The working process of an electric locomotive passing the neutral section in backward direction is contrary to the above process, and it is omitted here.

It can be seen that the proposed scheme helps the electric locomotive pass through the neutral section with power, and the neutral section voltage is switched three times. The phase changes of each switching process are respectively 19.1°, 20.8°, 19.1°, which are basically the same. Compared to the conventional thyristor-based schemes, the voltage switching process of the proposed scheme is smoother.

C. TOPOLOGY ANALYSIS

The voltage stress and the current stress of the four switches in the proposed scheme are concluded in TABLE 1. Therein, P_T is the rated power of a train.

TABLE 1. Voltage stress and current stress of the four switches in the proposed scheme.

	Voltage stress	Current stress
S_a, S_b	$0.667U_m$	$2.268P_T/U_m$
S_{c1}, S_{c2}	$0.333U_m$	$2.268P_T/U_m$

The total voltage stress of all switches is $2U_m$, which is the same as that of the conventional thyristor-based schemes. Since the voltage amplitude in the transition states is lowered to $0.882U_m$, the current stress is increased by 13% compared to the conventional schemes. Nonetheless, the current margin of all switching devices is generally 1.5 to 2 times of the rated current and the duration of the two transition states is relatively short. With the overcurrent capacity of thyristors, the increase of current stress has little impact on this scheme. It implies that although two additional switches are introduced into the proposed scheme, the total number of the switching devices is actually unchanged compared to the conventional schemes.

The auxiliary transformer T_a only works in the transition states. In this duration, the traction current of the train can be expressed as

$$I_T = \sqrt{2}P_T \Big/ (0.882U_m) = 1.603P_T/U_m \tag{4}$$

Correspondingly, the theoretical rated capacity of T_a can be calculated as

$$S_T = \frac{1}{3} \times \frac{U_m}{\sqrt{2}} \times \frac{1.603P_T}{U_m} = 0.378P_T \tag{5}$$

Further, since the operation time of T_a is only a few hundred microseconds, T_a is recommended to work at the

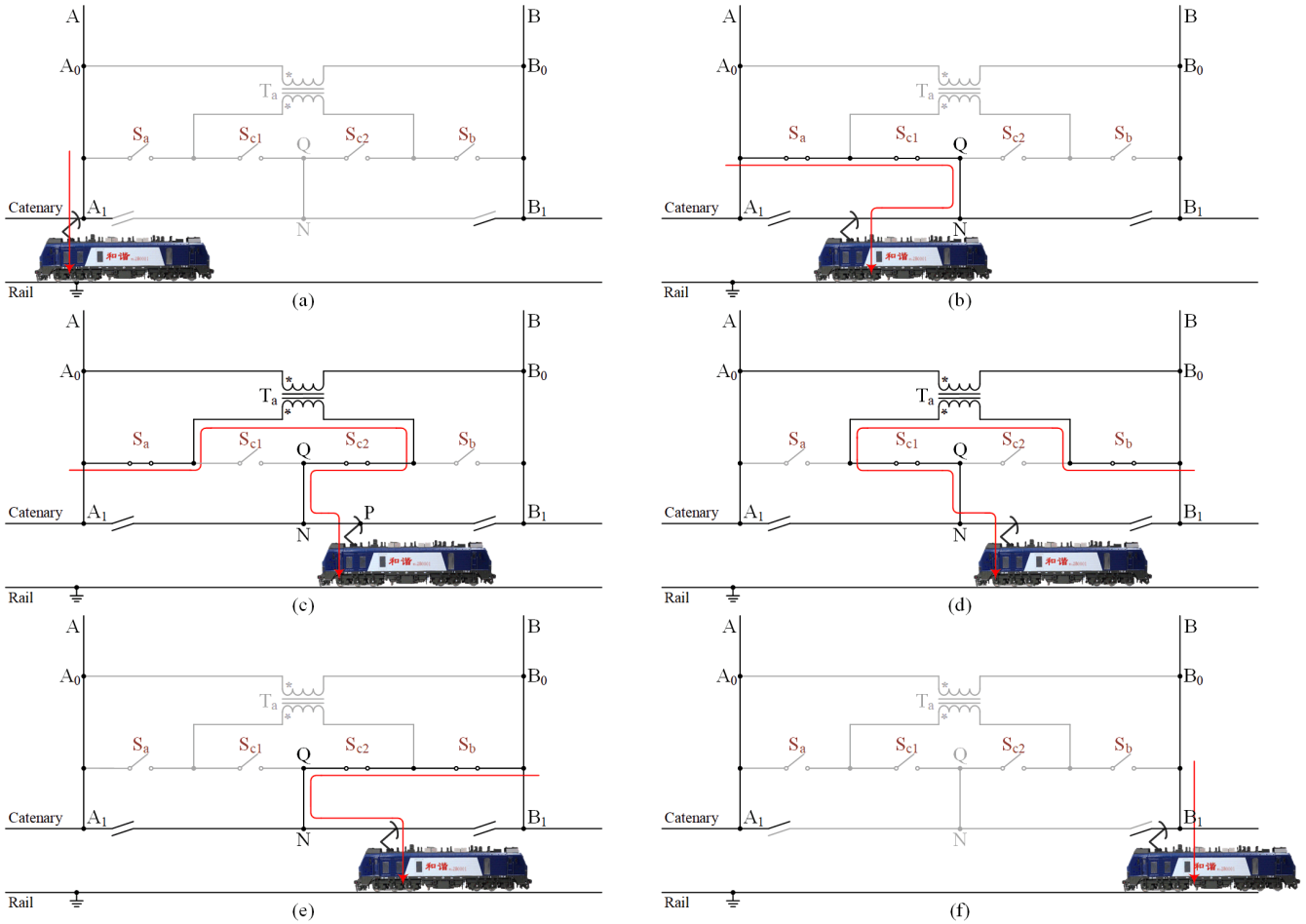

FIGURE 3. Different working states of the proposed scheme when an electric locomotive passing through the neutral section. (a) State I. (b) State II. (c) State III. (d) State IV. (e) State V. (f) State VI.

short-time overload state. Consequently, the rated capacity of T_a can be further lowered [20].

$$S'_T = S_T/1.5 = 0.252P_T \tag{6}$$

According to (6), the auxiliary transformer capacity of the proposed scheme is merely a quarter of P_T.

III. CHARACTERISTICS ANALYSIS

As shown in Fig. 2, the amplitudes of two transition voltages in the proposed scheme are lower than that of two feeders due to the construction idea, which will affect its application. On the other hand, the exciting current in the on-board transformer is a key factor that needs to be focused on for the switch-based scheme [21]. The two issues will be deeply discussed in this section.

A. SCHEME ADAPTABILITY

According to the analysis in Section II, when the phase difference between two power supply arms on both sides of a neutral section is 60°, both the amplitudes of the transition voltages, $\dot{U}_{n1}$ and $\dot{U}_{n2}$, are $0.882U_m$. Generally, the voltage fluctuation of the traction network has little impact on the electric locomotive since it is designed to function properly with reduced voltage by 24% or increased voltage by 10% than the rated voltage based on IEC-6850 and EN-50163. Nevertheless, if the voltages of two power supply arms are at a level close to the undervoltage protection threshold of 19 kV, the protection of the electric locomotive will be triggered with the proposed scheme. In other word, the allowed minimum voltage of the traction network is raised to 21.5 kV for the situation with 60° phase difference of two power supply arms.

However, when the phase difference between two power supply arms is greater than 60°, the situation will get worse. Fig. 4 shows the phasor diagram of the proposed scheme applied in the situation with 90° phase difference between two power supply arms.

In this condition, $\dot{U}_a$ and $\dot{U}_b$ should be expressed as

$$\begin{cases} \dot{U}_a = U_m\angle 0° \\ \dot{U}_b = U_m\angle -90° \end{cases} \tag{7}$$

Similarly, $\dot{U}_{n1}$ and $\dot{U}_{n2}$ can be calculated as

$$\begin{cases} \dot{U}_{n1} = 0.745U_m\angle -26.6° \\ \dot{U}_{n2} = 0.745U_m\angle -63.4° \end{cases} \tag{8}$$

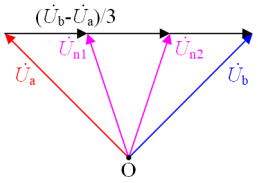

FIGURE 4. Phasor diagram of the proposed scheme applied in the situation with 90° phase difference of two power supply arms.

According to (8), the amplitudes of $\dot{U}_{n1}$ and $\dot{U}_{n2}$ are 0.745 times of $\dot{U}_a$ and $\dot{U}_b$. It means for the 25 kV traction power supply system, the effective value of the transition voltages is only 18.6 kV, which is lower than the undervoltage protection threshold. Therefore, the proposed scheme is not suitable for the case that the phase difference between two power supply arms is greater than or equal to 90°.

Based on the above analysis, the proposed scheme should be applied to the neutral section where the phase difference between two power supply arms on both sides is 60° and the traction network voltage can maintain a high level. Actually, the situation of the traction network voltage lower than 21.5 kV is rarely occurred. In contrast, a 60° phase change of the neutral section voltage is more likely to significantly impact the PLL of the 4QC and the on-board transformer. This is one of the important reasons why the scheme is proposed to evade the direct switching of the neutral section voltage between two power supply arms.

B. FLUX LINKAGE ANALYSIS

For the conventional thyristor-based schemes, it is hard to simultaneously consider the power interruption time of the electric locomotive and the exciting current of the on-board transformer. Besides, the flux linkage variation during the power interruption time is unpredictable, so the switching moments of these scheme are difficult to determine [22]. The experimental results of a conventional thyristor-based scheme are shown in Fig. 5. There is an inrush current of 762 A, which seriously affects the train operation.

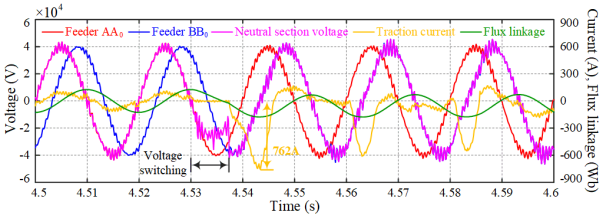

FIGURE 5. Experimental results of a conventional thyristor-based scheme.

For the proposed scheme, in order to minimize the dead time impact as much as possible and prevent a short circuit in the system, the dead time of each voltage switching is set to 300 μs. To simplify the analysis, the train is assumed to work at the unit power factor state, so the phases of the grid voltage and the input current are the same. Furthermore, the impact of the grid voltage on the flux linkage during the dead time is ignored.

Generally, the input voltage on the primary side of the on-board transformer can be expressed as

$$u_T(t) = U_m \sin(\omega_0 t + \alpha) \tag{9}$$

where ω_0 is the angular frequency of the power grid, α is the closing angle.

The flux linkage of the on-board transformer can be solved as

$$\psi(t) = -\psi_m \cos(\omega_0 t + \alpha) + (\psi_r + \psi_m \cos\alpha)\, e^{-t/\tau} \tag{10}$$

Therein, ψ_m is the rated flux linkage that equals to U_m/ω_0, ψ_r is the remanence of the on-board transformer, τ is the time constant.

According to (10), the maximum flux linkage after the voltage switching is approximate to

$$\psi_{max} \approx \psi_m + |\psi_r + \psi_m \cos\alpha| \tag{11}$$

The situation of a train passing through the neutral section from AA_0 to BB_0 is analyzed firstly. Before the train arrives at point P shown in Fig. 3(c), the neutral section voltage is $\dot{U}_a$. At this time, the maximum flux linkage of the on-board transformer is ψ_m.

When the train arrives at point P, S_{c1} is switched off and then S_{c2} is switched on after 300 μs. Let S_{c1} be switched off when $\dot{U}_n$ crosses zero in the negative direction, so the remanence of the on-board transformer is ψ_m and the closing angle of S_{c2} in this duration is

$$\alpha_1 = 180° - 19.1° + \frac{300\mu s}{20ms} \times 360° = 166.3° \tag{12}$$

According to (11), the maximum flux linkage of the on-board transformer in the first transition state is

$$\psi_{max1} \approx 0.882\psi_m + |\psi_m + 0.882\psi_m \cos\alpha_1| = 1.03\psi_m \tag{13}$$

After a few line-frequency cycles, the 4QCs recovers to the unit power factor state. S_a and S_{c2} are switched off firstly, and then S_b and S_{c1} are switched on after 300 μs. Let S_a and S_{c2} be switched off when $\dot{U}_n$ crosses zero in the positive direction, so the remanence of the on-board transformer is

$$\psi_{r1} \approx -0.882\psi_m + (\psi_m + 0.882\psi_m \cos\alpha_1) = -0.74\psi_m \tag{14}$$

The closing angle of S_b and S_{c1} in this duration is

$$\alpha_2 = 360° - (40.9° - 19.1°) + \frac{300\mu s}{20ms} \times 360° = 343.6° \tag{15}$$

In the second transition state, the maximum flux linkage is

$$\psi_{max2} \approx 0.882\psi_m + |\psi_{r1} + 0.882\psi_m \cos\alpha_2| = 0.99\psi_m \tag{16}$$

Similarly, after a few line-frequency cycles again, S_{c1} is switched off and then S_{c2} is switched on after 300 μs.

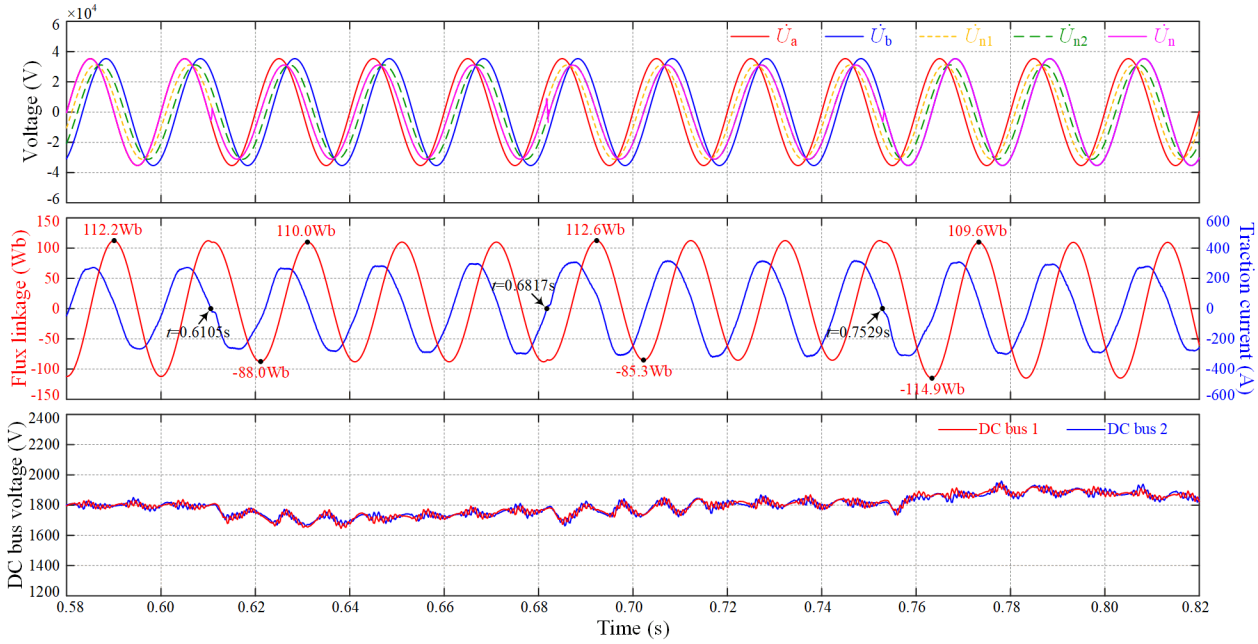

FIGURE 6. Simulation results of the voltage switching process when a train is from feeder AA_0 to feeder BB_0.

Let S_{c1} is switched off when $\dot{U}_n$ crosses zero in the negative direction, so the remanence of the on-board transformer is

$$\psi_{r2} \approx \psi_{max2} = 0.99\psi_m \tag{17}$$

The closing angle of S_{c2} in this duration is

$$\alpha_3 = 180° - 19.1° + \frac{300\mu s}{20ms} \times 360° = 166.3° \tag{18}$$

After the voltage switching, the maximum flux linkage is

$$\psi_{max3} \approx \psi_m + |\psi_{r2} + \psi_m \cos\alpha_3| = 1.02\psi_m \tag{19}$$

Based on the above analysis, the flux linkage of the on-board transformer during the entire switching process will not be larger than $1.03\psi_m$. Since the saturation flux linkage is generally 1.2 times of ψ_m, there is no inrush current. With the same analytical method, the maximum flux linkage of the on-board transformer when a train passes through the neutral section from BB_0 to AA_0 is $1.08\psi_m$, which is also lower than the saturation flux linkage. Therefore, the inrush current can be well suppressed by the proposed scheme.

IV. SIMULATION RESULTS

A simulation model based on MATLAB/Simulink referring to the electrical parameters of a HXD_1 electric locomotive as shown in TABLE 2 is built to demonstrate the correctness of the above theoretical analysis.

Fig. 6 shows the simulation results of the voltage switching process when a train is from AA_0 to BB_0, which include $\dot{U}_a$, $\dot{U}_b$, $\dot{U}_{n1}$, $\dot{U}_{n2}$, $\dot{U}_n$, the flux linkage of the on-board transformer, the traction current, and the DC bus voltages. Before the voltage switching, the maximum flux linkage of the on-board transformer is 122.2 Wb, which is the rated value. Firstly, at 0.6105 s, the traction current crosses zero in the negative direction and $\dot{U}_n$ is switched from $\dot{U}_a$ to $\dot{U}_{n1}$ after 300 μs. In the first transition state, the maximum flux linkage is 110.0Wb. Subsequently, within approximately 3.5 line-frequency cycles, the 4QCs are back to the steady state. At 0.6817 s, the traction current crosses zero in the positive direction, $\dot{U}_n$ is switched from $\dot{U}_{n1}$ to $\dot{U}_{n2}$. In the second transition state, the maximum flux linkage is 112.6 Wb. After the 4QCs returns to the steady state within 3.5 line-frequency cycles again, at 0.7529 s, the traction current crosses zero in the negative direction, and $\dot{U}_n$ is switched from $\dot{U}_{n2}$ to $\dot{U}_b$. In this state, the maximum flux linkage is 114.9 Wb. Subsequently, it will gradually decay to the rated value.

Based on the simulation results, the maximum flux linkage of the on-board transformer in the whole process is 114.9 Wb, which is 1.02 times of the rated value. Consequently, it will not generate an inrush current. In addition, according to the waveforms of the DC bus voltages, the voltage fluctuation

TABLE 2. Main electrical parameters of the simulation model.

Parameters	Values	Parameters	Values
Rated power	4.8 MW	Grid frequency	50 Hz
Voltage of AA_0	25 kV	Voltage of BB_0	25 kV
Phase of AA_0	0°	Phase of BB_0	-60°
Turns ratio of on-board transformer	25000:970	Turns ratio of auxiliary transformer	3:1
Inductance of 4QCs	0.817 mH	Capacitance in DC side	12 mF
2nd resonant inductance	0.27 mH	2nd resonant capacitance	9.85 mF
Voltage in DC side	1800 V	Load in DC side	1.35 Ω

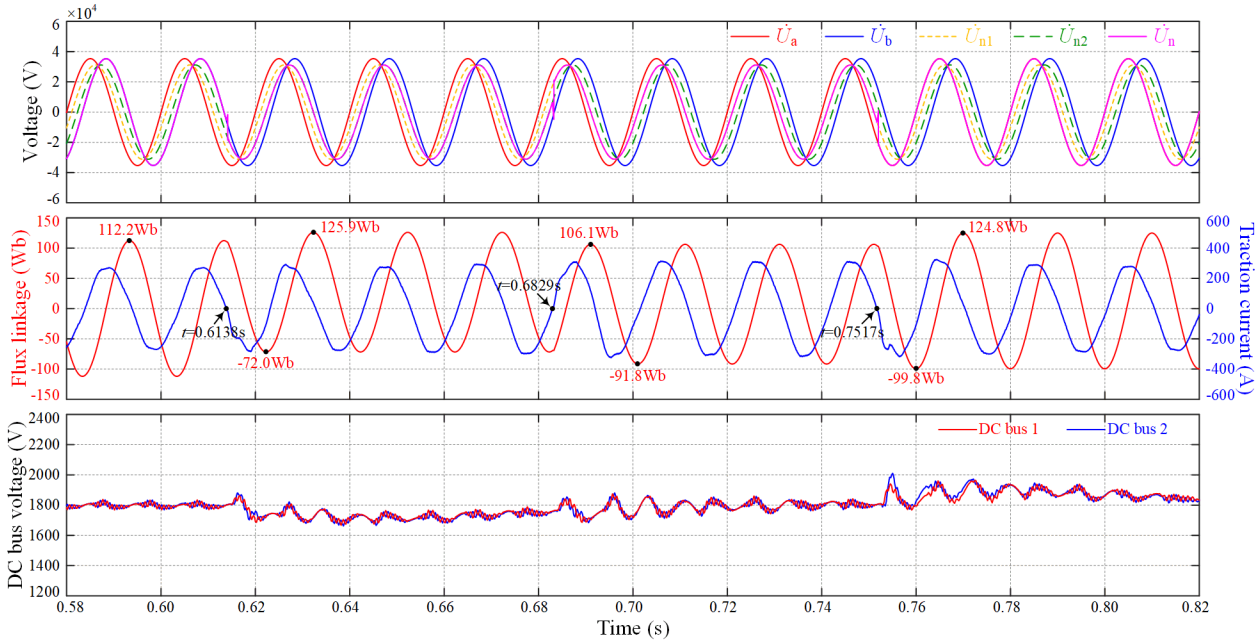

FIGURE 7. Simulation results of the voltage switching process when a train is from feeder BB_0 to feeder AA_0.

TABLE 3. Comparison results of the conventional thyristor-based schemes, the proposed scheme, and the scheme in [20].

	Number of switches	Total voltage stress	Current stress	Number of auxiliary transformers	Capacity of auxiliary transformers	Phase change	Power interruption	Maximum flux linkage
Conventional schemes	2	$2U_m$	$2P_T/U_m$	0	——	60°	≥3.3ms	Unpredictable
Proposed scheme	4	$2U_m$	$2.268P_T/U_m$	1	$0.252P_T$	19.1°, 21.8°, 19.1°	900μs	$1.12\psi_m$
Scheme in [20]	6	$2.536U_m$	$2P_T/U_m$	2	$0.263P_T$	20°, 20°, 20°	900μs	$1.15\psi_m$

caused by the voltage switching is small and the later traction drive system will not be affected.

The simulation results of the voltage switching process when a train is from BB_0 to AA_0 are shown in Fig. 7. According to Fig. 7, the maximum flux linkage of the on-board transformer during the reverse voltage switching process occurs when $\dot{U}_n$ is switched from $\dot{U}_b$ to $\dot{U}_{n2}$. It is about 125.9 Wb and 1.12 times of the rated value, which is in the acceptable range. Meanwhile, the fluctuation of the DC bus voltages is acceptable, so the train operation will not be affected.

The simulation results indicate an excellent working effect of the proposed scheme. When a train passes through the neutral section, the total power interruption time is only 900 μs and the flux linkage of the on-board transformer is always within the accepted range. Therefore, the voltage switching process will not affect the traction drive system of the electric locomotive.

According to the above analysis, the comparison results of the conventional thyristor-based schemes, the proposed scheme, and the scheme in [20] are concluded in TABLE 3. Therein, the necessary switching devices of different schemes are represented by the total voltage stress.

Compared to the conventional thyristor-based schemes, the total number of the switching devices is actually unchanged and only one auxiliary transformer with the capacity of $0.252P_T$ is added in the proposed scheme. As a result, the increased cost brought by the proposed scheme is limited to a certain extent. In addition, the power interruption time is shortened by the proposed scheme from 3.3ms in the conventional thyristor-based schemes to 900 μs. On the other hand, the proposed scheme has fewer switching devices, smaller number and capacity of the auxiliary transformers, and less flux linkage of the on-board transformer compared to the scheme in [20]. Therefore, the proposed scheme has much lower cost and simpler structure with a similar working effect.

V. EXPERIMENTAL VERIFICATION

To further verify the feasibility and effectiveness of the proposed scheme, a scaled-down experimental platform is established in the lab. As shown in Fig. 8, the experimental platform is connected to the three-phase civilian power grid

TABLE 4. Main electrical parameters of the experimental prototype.

Parameters	Values/Models	Parameters	Values/Models
Voltage of feeder A	380 V	Voltage of feeder B	380 V
Phase of feeder A	0°	Phase of feeder B	-60°
Turns ratio of auxiliary transformer	3:1	Capacity of auxiliary transformer	2 kVA
Turns ratio of on-board transformer	1:1	Capacity of on-board transformer	10 kVA
Inductance of 4QC	4.7 mH	Capacitance in DC side	2.42 mF
Voltage of DC bus	600 V	Load in DC side	60 Ω
2nd resonant inductance	2.3 mH	2nd resonant capacitance	1.1 mF
Device of S_a, S_b, S_{c1}, S_{c2}	BTW69-1200N	Switching device of 4QC	IMZ120R030M1H
Switching frequency of 4QC	5 kHz	Control frequency of 4QC	10 kHz

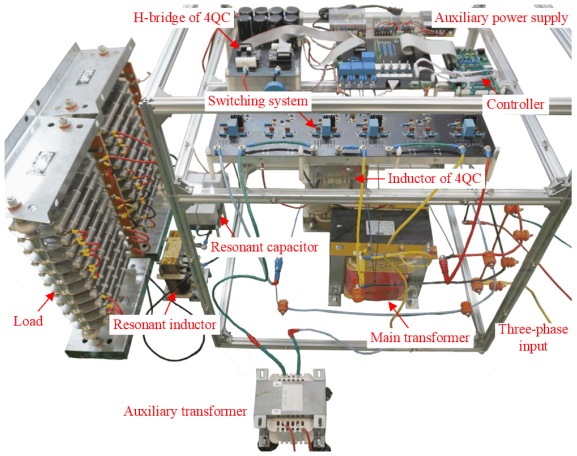

FIGURE 8. Scaled-down experimental platform.

and two line-voltages are used to simulate the feeder A and the feeder B. The train load is substituted by a 1:1 two-winding transformer with a 4QC. A 60 Ω resistor load is connected to the DC side and the rated experimental power is 6 kW. The switching frequency of the H-bridge is set to 5 kHz, while the control frequency is 10 kHz with the single-polar sine pulse width modulation of frequency doubled technology for reducing the current harmonics. The detailed electrical parameters are listed in TABLE 4.

A. FORWARD SWITCHING PROCESS

Fig. 9 shows the experimental results when the input voltage of the experimental platform is switched from the leading phase to the lagging phase. The voltage of feeder A and the voltage of feeder B are respectively represented by u_a and u_b. u_T and i_T are the input voltage and current. The process of u_T switching from u_a to the first transition voltage is shown in Fig. 9(a). At the beginning, u_T equals to u_a. The 4QC is in the unit power factor state thanks to the voltage and current double closed-loop control. At this time, the peak flux linkage of the on-board transformer is calculated as 1.642 Wb with the integral calculation of u_T. When i_T crosses zero in the negative direction, u_T is switched to the first transition state.

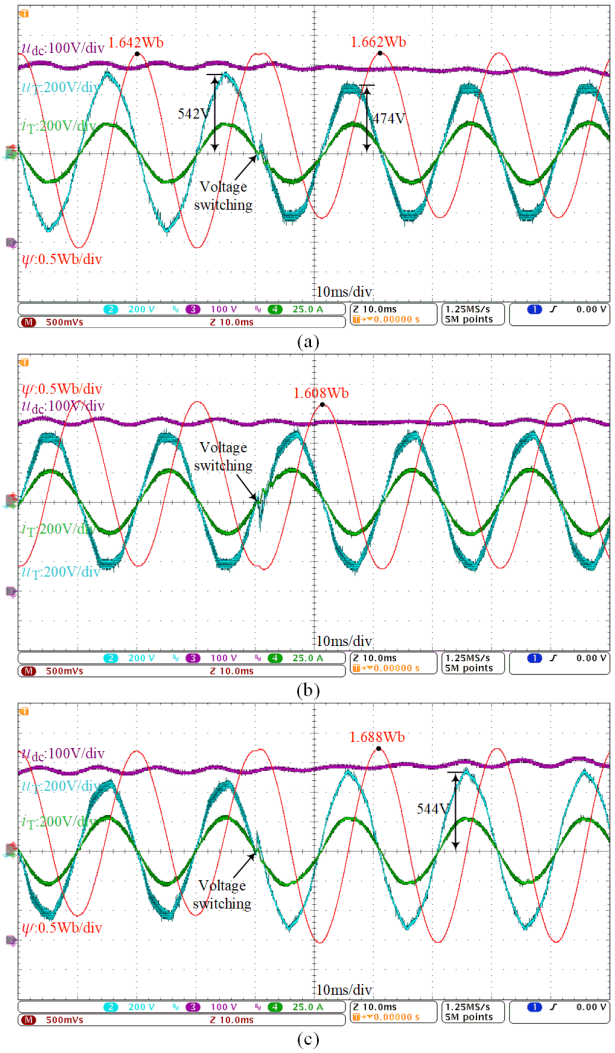

FIGURE 9. Experimental results when u_T is switched from u_a to u_b. Process of u_T switched from (a) u_a to the first transition voltage, (b) the first transition voltage to the second transition voltage, and (c) the second transition voltage to u_b.

It can be seen that the amplitude of u_T decreases from 542 V to 474 V. In this state, the maximum flux linkage is 1.662 Wb. Within about 100 ms, the 4QC returns to the unit power

factor state. Then u_T is switched to the second transition state. As shown in Fig. 9(b), the maximum flux linkage in this state is 1.608 Wb. After 100 ms again, u_T is switched to u_b. According to Fig. 9(c), the amplitude of u_T recovers to 544 V and the maximum flux linkage is 1.688 Wb. It can be seen that the maximum flux linkage in the whole switching process is 1.688Wb, which is 1.03 times of the rated value. The experimental results are in accordance with the theoretical analysis. In addition, the DC bus voltage u_{dc} is stable and the impact of the voltage switching process on the 4QC can be ignored.

B. REVERSE SWITCHING PROCESS

Fig. 10 illustrates the experimental results during the reverse switching process. It is opposite to that of Fig. 9 and the duration of each transition state is also approximately 100 ms. According to Fig. 10, the peak flux linkage of the on-board transformer is 1.652 Wb before the voltage switching. Then the flux linkage is up to 1.804 Wb after u_T is switched to u_a. Consequently, the maximum flux linkage when the input voltage of the on-board transformer is switched from the lagging phase to the leading phase is 1.09 times of the rated value. Similarly, u_{dc} remains unaffected during this process.

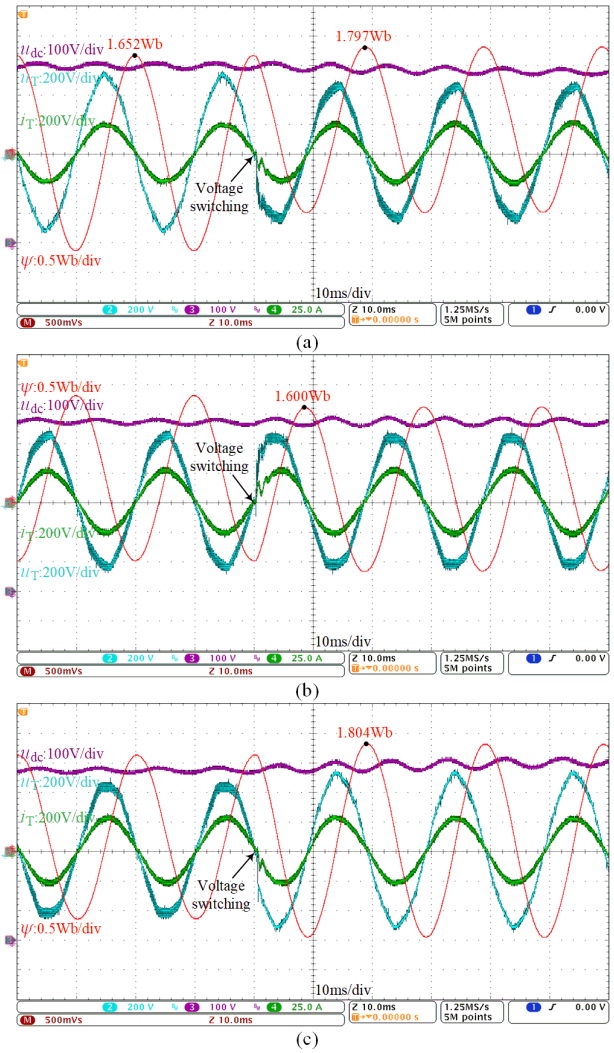

FIGURE 10. Experimental results when u_T is switched from u_b to u_a. Process of u_T switched from (a) u_b to the second transition voltage, (b) the second transition voltage to the first transition voltage, and (c) the first transition voltage to u_a.

VI. CONCLUSION

A modified thyristor-based auto-passing neutral section scheme with one simplified auxiliary transformer is proposed in this paper. With the cooperation of one 3:1 transformer and two additional switches, two transition voltages, whose phases are between that of two power supply arms, are introduced. Then the neutral section voltage can be switched step by step within a small phase change between the two power supply arm voltages. Compared to the conventional thyristor-based schemes, the voltage switching process is smoother and the power interruption time of the train can be further shortened to 900 μs. Meanwhile, the flux linkage of the on-board transformer is kept in 1.12 times of the rated value during the whole switching process, so that the issue of the inrush current can be solved. Furthermore, the proposed scheme has much simpler structure and higher economy than that in [20] with a similar working effect.

On the other hand, since the amplitudes of two transition voltages will be reduced according to the construction idea, the proposed scheme is not suitable for the application that the phase difference between two power supply arms on both sides of the neutral section is greater than or equal to 90°. Nevertheless, it has an excellent working effect for the application of 60° phase difference based on the simulation and experimental results. The influence of the neural section on the train can be significantly suppressed by the proposed scheme.

REFERENCES

[1] I. Krastev, P. Tricoli, S. Hillmansen, and M. Chen, "Future of electric railways: Advanced electrification systems with static converters for AC railways," *IEEE Electrific. Mag.*, vol. 4, no. 3, pp. 6–14, Sep. 2016.

[2] A. D. Femine, D. Gallo, D. Giordano, C. Landi, M. Luiso, and D. Signorino, "Power quality assessment in railway traction supply systems," *IEEE Trans. Instrum. Meas.*, vol. 69, no. 5, pp. 2355–2366, May 2020.

[3] C. Yang, F. Zhu, Y. Yang, N. Lu, and X. Dong, "Modeling of catenary electromagnetic emission with electrified train passing through neutral section," *Int. J. Electr. Power Energy Syst.*, vol. 147, May 2023, Art. no. 108899.

[4] H. Hayashiya and K. Ajiki, "Closing surge and surge propagation at SHINKANSEN changeover section," *IEEJ Trans. Ind. Appl.*, vol. 126, no. 3, pp. 322–329, 2006.

[5] S. Midya, D. Bormann, T. Schutte, and R. Thottappillil, "Pantograph arcing in electrified railways—Mechanism and influence of various parameters—Part II: With AC traction power supply," *IEEE Trans. Power Del.*, vol. 24, no. 4, pp. 1940–1950, Oct. 2009.

[6] K. Huang, Z. Liu, and X. Li, "Research on electromagnetic transient processes of long marshalling high-speed train passing articulated split-phase region," *IEEE Access*, vol. 7, pp. 78597–78615, 2019.

[7] H.-S. Shin, S.-M. Cho, and J.-C. Kim, "Protection scheme using SFCL for electric railways with automatic power changeover switch system," *IEEE Trans. Appl. Supercond.*, vol. 22, no. 3, pp. 5600604–5600604, Jun. 2012.

[8] E. Delgado, I. Aizpuru, J. M. Canales, M. Ayarzaguena, A. Galparsoro, and T. Nieva, "Static switch based solution for improvement of neutral sections in HSR systems," in *Proc. Electr. Syst. Aircr., Railway Ship Propuls.*, Oct. 2012, pp. 1–6.
[9] Z. Zhang, T. Q. Zheng, K. Li, R. Hao, X. You, Z. Zhang, and J. Yang, "Smart electric neutral section executer embedded with automatic pantograph location technique based on voltage and current signals," *IEEE Trans. Transport. Electrific.*, vol. 6, no. 3, pp. 1355–1367, Sep. 2020.
[10] X. Tian, Q. Jiang, and Y. Wei, "Research on novel uninterruptible phase-separation passing scheme in electrified railways," *Power Syst. Protection Control*, vol. 40, no. 21, pp. 14–18, Nov. 2012.
[11] S. Cheng, C. Liu, T. Yu, C. Xiang, P. Tian, K. Li, and X. Wu, "Structure improvement and control algorithm optimization-based ground automatic neutral-section passing method for train," *IEEE Trans. Emerg. Sel. Topics Power Electron.*, vol. 11, no. 3, pp. 2879–2894, Jun. 2023.
[12] X. Tian, Q. Jiang, and Y. Wei, "Research on novel railway uninterruptible flexible connector with series-connected transformers and back-to-back converter," in *Proc. IEEE ECCE Asia Downunder*, Jun. 2013, pp. 111–116.
[13] Z. Li, X. Li, Y. Lin, Y. Wei, Z. Li, Z. Li, and C. Lu, "Active disturbance rejection control for static power converters in flexible AC traction power supply systems," *IEEE Trans. Energy Convers.*, vol. 37, no. 4, pp. 2851–2862, Dec. 2022.
[14] J. Yuan, Z. Ni, F. Xiao, and Y. Min, "Study on the control method and the uninterrupted phase-separation passing system with voltage compensation function," *Trans. China Electrotech. Soc.*, vol. 26, no. 5, pp. 1084–1095, 2021.
[15] Z. Ni, J. Yuan, F. Xiao, L. Peng, Z. Zhang, and Y. Min, "Multi-function uninterrupted phase-separation passing system and its control method," *CSEE J. Power Energy Syst.*, vol. 9, no. 6, pp. 2332–2343, Nov. 2023.
[16] M. Chen, Q. Li, C. Roberts, S. Hillmansen, P. Tricoli, N. Zhao, and I. Krastev, "Modelling and performance analysis of advanced combined co-phase traction power supply system in electrified railway," *IET Gener., Transmiss. Distribution*, vol. 10, no. 4, pp. 906–916, Mar. 2016.
[17] X. He, Z. Shu, X. Peng, Q. Zhou, Y. Zhou, Q. Zhou, and S. Gao, "Advanced cophase traction power supply system based on three-phase to single-phase converter," *IEEE Trans. Power Electron.*, vol. 29, no. 10, pp. 5323–5333, Oct. 2014.
[18] Z. Zhang, T. Q. Zheng, C. Gao, K. Li, and J. Guo, "An automatic neutral section power supplier serving as railway power conditioner on time-division basis," *IEEE Trans. Power Electron.*, vol. 39, no. 8, pp. 9329–9343, Aug. 2024.
[19] S. M. M. Gazafrudi, A. T. Langerudy, E. F. Fuchs, and K. Al-Haddad, "Power quality issues in railway electrification: A comprehensive perspective," *IEEE Trans. Ind. Electron.*, vol. 62, no. 5, pp. 3081–3090, May 2015.
[20] Z. Zhang, K. Li, Z. Zhang, T. Q. Zheng, R. Hao, and X. You, "A thyristor-based auto-passing neutral section scheme with auxiliary transformers for AC electrified railway," *IEEE Trans. Transport. Electrific.*, vol. 9, no. 2, pp. 2296–2307, Jun. 2023.
[21] S. Wang, L. Zhang, G. Yu, E. Dong, J. Zou, Y. Cong, and Y. Tian, "Hybrid phase-controlled circuit breaker with switch system used in the railway auto-passing neutral section with an electric load," *CSEE J. Power Energy Syst.*, vol. 5, no. 4, pp. 545–552, Dec. 2019.
[22] Z. Zhang, K. Li, Z. Zhang, T. Q. Zheng, R. Hao, and X. You, "Ground auto-passing neutral section scheme based on IGCT and its voltage switching control strategy," *Power Syst. Technol.*, vol. 47, no. 11, pp. 4801–4809, 2023.

ZHI ZHANG (Member, IEEE) was born in Anhui, China, in 1994. He received the B.S. and Ph.D. degrees in electrical engineering from Beijing Jiaotong University, Beijing, China, in 2016 and 2022, respectively.

He is currently an Assistant Research Fellow with the Locomotive & Car Research Institute, China Academy of Railway Sciences Corporation Ltd., Beijing. His current research interests include railway electrification systems and PWM converter.

TRILLION Q. ZHENG (Senior Member, IEEE) received the B.S. degree in electrical engineering from Southwest Jiaotong University, Sichuan, China, in 1986, and the M.S. and Ph.D. degrees in electrical engineering from Beijing Jiaotong University, Beijing, China, in 1992 and 2002, respectively.

He is currently an University Distinguished Professor with Beijing Jiaotong University, where he is also the Director of the Center for Electric Traction, funded by Ministry of Education, China. His current research interests include the power supplies and AC drives of railway traction systems, high-performance and low-loss power electronics systems, PV-based converters and control, active power filters, and power quality correction.

Prof. Zheng received the Youth Award of Railway Science and Technology of Zhan Tianyou, in 2005, and the Zhongda Scholar for Power Electronics and Motor Drive area by the Delta Environmental and Educational Foundation, in 2007.

ZHIBO ZHANG (Graduate Student Member, IEEE) was born in Tieling, China, in 1996. He received the B.S. degree in electrical engineering from Beijing Jiaotong University, Beijing, China, in 2019, where he is currently pursuing the Ph.D. degree in power electronics with the School of Electrical Engineering. His current research interests include railway electrification systems and PWM converter.

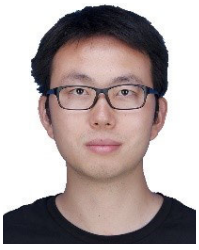

KAI LI (Member, IEEE) received the B.S. degree in electrical engineering from Wuhan University, Wuhan, Hubei, China, in 2011, and the Ph.D. degree from Tsinghua University, Beijing, China, in 2017.

He was a Visiting Scholar with the Center for Power Electronics Systems, Virginia Tech, Blacksburg, VA, USA, from 2013 to 2015. He was a Postdoctoral Fellow with Tsinghua University, from 2017 to 2019. In 2019, he joined the School of Electrical Engineering, Beijing Jiaotong University, Beijing, where he is currently an Associate Professor with the School of Electrical Engineering. His current research interests include solid-state transformer, railway electrification systems, modular multilevel converters, and electrolytic hydrogen production converters.

SILE YANG received the B.S. and M.S. degrees in automation science and electrical engineering from Beihang University, Beijing, China, in 2008 and 2012, respectively.

He is currently an Associate Research Fellow with the Locomotive & Car Research Institute, China Academy of Railway Sciences Corporation Ltd., Beijing. His current research interests include railway electrification systems and high voltage technology.